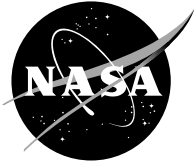NASA/TM—2001-211082 AIAA–2001–2581

Multiobjective Optimization of Rocket Engine Pumps Using Evolutionary Algorithm

Akira Oyama
Ohio Aerospace Institute, Brook Park, Ohio

Meng-Sing Liou
Glenn Research Center, Cleveland, Ohio

August 2001

The NASA STI Program Office . . . in Profile

Since its founding, NASA has been dedicated to the advancement of aeronautics and space science. The NASA Scientific and Technical Information (STI) Program Office plays a key part in helping NASA maintain this important role.

The NASA STI Program Office is operated by Langley Research Center, the Lead Center for NASA's scientific and technical information. The NASA STI Program Office provides access to the NASA STI Database, the largest collection of aeronautical and space science STI in the world. The Program Office is also NASA's institutional mechanism for disseminating the results of its research and development activities. These results are published by NASA in the NASA STI Report Series, which includes the following report types:

- TECHNICAL PUBLICATION. Reports of completed research or a major significant phase of research that present the results of NASA programs and include extensive data or theoretical analysis. Includes compilations of significant scientific and technical data and information deemed to be of continuing reference value. NASA's counterpart of peer-reviewed formal professional papers but has less stringent limitations on manuscript length and extent of graphic presentations.

- TECHNICAL MEMORANDUM. Scientific and technical findings that are preliminary or of specialized interest, e.g., quick release reports, working papers, and bibliographies that contain minimal annotation. Does not contain extensive analysis.

- CONTRACTOR REPORT. Scientific and technical findings by NASA-sponsored contractors and grantees.

- CONFERENCE PUBLICATION. Collected papers from scientific and technical conferences, symposia, seminars, or other meetings sponsored or cosponsored by NASA.

- SPECIAL PUBLICATION. Scientific, technical, or historical information from NASA programs, projects, and missions, often concerned with subjects having substantial public interest.

- TECHNICAL TRANSLATION. English-language translations of foreign scientific and technical material pertinent to NASA's mission.

Specialized services that complement the STI Program Office's diverse offerings include creating custom thesauri, building customized data bases, organizing and publishing research results . . . even providing videos.

For more information about the NASA STI Program Office, see the following:

- Access the NASA STI Program Home Page at *http://www.sti.nasa.gov*

- E-mail your question via the Internet to help@sti.nasa.gov

- Fax your question to the NASA Access Help Desk at 301–621–0134

- Telephone the NASA Access Help Desk at 301–621–0390

- Write to:
  NASA Access Help Desk
  NASA Center for AeroSpace Information
  7121 Standard Drive
  Hanover, MD 21076

NASA/TM—2001-211082 AIAA–2001–2581

Multiobjective Optimization of Rocket Engine Pumps Using Evolutionary Algorithm

Akira Oyama
Ohio Aerospace Institute, Brook Park, Ohio

Meng-Sing Liou
Glenn Research Center, Cleveland, Ohio

National Aeronautics and
Space Administration

Glenn Research Center

Acknowledgments

Available from

NASA Center for Aerospace Information
7121 Standard Drive
Hanover, MD 21076

National Technical Information Service
5285 Port Royal Road
Springfield, VA 22100

Available electronically at http://gltrs.grc.nasa.gov/GLTRS

MULTIOBJECTIVE OPTIMIZATION OF ROCKET ENGINE PUMPS
USING EVOLUTIONARY ALGORITHM

Akira Oyama
Ohio Aerospace Institute
Cleveland, Ohio 44142
440–962–3148, aoyama@dino.grc.nasa.gov

Meng-Sing Liou
National Aeronautics and Space Administration
Glenn Research Center
Cleveland, Ohio 44135
216–433–5855, meng-sing.liou@grc.nasa.gov

ABSTRACT

A design optimization method for turbopumps of cryogenic rocket engines has been developed. Multiobjective Evolutionary Algorithm (MOEA) is used for multiobjective pump design optimizations. Performances of design candidates are evaluated by using the meanline pump flow modeling method based on the Euler turbine equation coupled with empirical correlations for rotor efficiency.

To demonstrate the feasibility of the present approach, a single stage centrifugal pump design and multistage pump design optimizations are presented. In both cases, the present method obtains very reasonable Pareto-optimal solutions that include some designs outperforming the original design in total head while reducing input power by 1%. Detailed observation of the design results also reveals some important design criteria for turbopumps in cryogenic rocket engines. These results demonstrate the feasibility of the EA-based design optimization method in this field.

INTRODUCTION

While the budget for space development programs has drastically shrunk in most countries, recent and future space missions increasingly demand high performance and reliable rocket engine systems and components, such as turbopumps. Progress in computational fluid dynamics (CFD) methods and development of powerful computational facilities have contributed to the reduction in required cost and time to develop advanced turbopump designs. The design process still largely depends on experienced designers. Therefore, numerical design methods coupled with CFD, which are capable of efficiently developing advanced turbopump designs, can greatly reduce such dependency.

Among numerical optimization algorithms, gradient-based methods are long-standing and most widely used approaches[1-3]. These methods use the gradient of an objective function with respect to changes in design variables to calculate a search direction using steepest descent, conjugate gradient, quasi Newton techniques, or adjoint formulations. The solution obtained by these methods will be a global optimum, only if the objective and constraints are differentiable and convex[4]. Unfortunately, the distribution of an objective function of real-world design problems is usually multimodal and one could only hope for a local optimum neighboring the initial design point. Therefore, to determine the global optimum, one must optimize from a number of initial points and check for consistency in the optima obtained. In this sense, the gradient-based methods are not robust.

Evolutionary Algorithms (EAs, for example, see [5]) are emerging design optimization algorithms modeled on the mechanism of natural evolution. EAs search from multiple points, instead of moving from a single point. In addition, they require no derivatives or gradients of the objective function. These features lead to robustness and simplicity in coupling with any evaluation codes. Parallel efficiency also becomes very high by using a simple master-slave concept for function evaluations, if such evaluations consume most of CPU time. Design optimization using CFD is a typical case. Application of EAs to multiobjective design problems is also straightforward because EAs maintain a population of design candidates in parallel. Due to these advantages, EAs are unique and attractive approach to real-world design optimization problems. Recently, EAs have been successfully applied to aerospace design optimization problems[5-9].

The objective of the present study is to develop and demonstrate a design optimization method for turbopumps used in the cryogenic rocket engines. The Multiobjective Evolutionary Algorithm (MOEA) will be used for multiobjective optimization of pump designs. Performances of design candidates will be evaluated by using the meanline pump flow modeling method based on the Euler turbine equation coupled with empirical correlations for rotor efficiency. Present approach will be applied to centrifugal and multistage turbopump design optimization problems.

EVOLUTIONARY ALGORITHMS

EAs mimic mechanism of natural evolution, where a biological population evolves over generations to adapt to an environment by selection according to fitness, recombination and mutation of genes (Fig.1). When EAs are applied to optimization problems, individual, fitness, and genes usually correspond to a design candidate, an objective function value, and design variables, respectively. One of the key features of EAs is that it searches from multiple points in the design space, instead of moving from a single point like gradient-based methods do. Furthermore, these methods work on function evaluations alone and do not require derivatives or gradients of the objective function. These features lead to the following advantages:

1) Robustness: EAs have capability of finding a global optimum, because they don't use function gradients that direct the search toward a local optimum. In addition, EAs have capability to handle any design problems that may involve non-differentiable objective function and/or a mix of continuous, discrete, and integer design parameters.

2) Capability of sampling various Pareto-optimal solutions in parallel: Real-world design optimization problems typically involve multiple and often competing objectives. The solution to such problem is not a unique optimal solution, but a set of compromised solutions, largely known as Pareto-optimal solutions. Each of those solutions is optimal in the sense that no improvement can be achieved in one objective component that does not lead to degradation in at least one of the remaining components. Therefore, primary goal of a multiobjective optimization problem is, unlike that of a single objective optimization, to find various Pareto-optimal solutions to show the precise tradeoff information among the completing objectives. By maintaining a population of solutions and introducing the concept of Pareto-optimality, EAs can uniformly sample various Pareto-optimal solutions in parallel.

3) Suitability to parallel computing: Since EAs are population-based search algorithms, all design candidates in each generation can be evaluated in parallel by using the simple master-slave concept. Parallel efficiency is also very high, if objective function evaluations consume most of CPU time.

4) Simplicity in coupling evaluation codes: As these methods use only objective function values of design candidates, EAs do not need substantial modification or sophisticated interface to evaluation codes. If an all-out re-coding were required to every optimization problem like the adjoint methods, extensive validation of the new code would be necessary every time. EAs can save such troubles.

The present MOEA uses floating-point representation, where an individual is characterized by a vector of real numbers. It is natural to use the floating-point representation for real parameter optimization problems instead of binary representation because it is conceptually closest to the real design space, and moreover, the string length is reduced to the number of design variables. Fonseca's Pareto-based ranking method[10] is used for fitness assignment where an individual's rank corresponds to the number of individuals in the current population that are better than the corresponding individual in every objective function. To maintain diversity in the population, a standard sharing function[10] is incorporated. As the elitism, the best-N selection[11] is incorporated, where the best N individuals are selected for the next generation among N parents and N children based on Pareto-optimality[5] so that the Pareto-optimal solutions will be kept once they are formed. Parents are selected from the best N individuals randomly. To generate new design candidates from these parents, the blended crossover (BLX-α) is used, which is the most common approach for recombination of two parents represented by a vector of real numbers proposed by Eshelman and Schaffer[12]. In this approach, children are generated on a segment defined by two parents, but the segment may be extended equally on both sides determined by a user specified parameter α. Thus, a child solution is expressed as:

$$Child1 = \gamma \cdot Parent1 + (1-\gamma) \cdot Parent2 \quad (1)$$
$$Child2 = (1-\gamma) \cdot Parent1 + \gamma \cdot Parent2 \quad (2)$$

where

$$\gamma = (\,1 + 2\alpha\,)\,u - \alpha \quad\quad (3)$$

Child1, *Child2* and *Parent1*, *Parent2* denote design parameters of the children and parents, respectively. *u* is uniform random number in [0,1]. Schematic view of BLX-α is shown in Fig. 2. When an EA is applied to a design optimization problem, what is important is balance of two conflicting goals: exploiting good

solutions and exploring the search space[13]. Thus, BLX-0.5 is used in which both exploration and exploitation are carried out equally. Since the strong elitism is used, high mutation rate of 0.2 is applied and a random disturbance is added to the parameter in the amount up to $\pm 20\%$ of the design space. Population size and maximum number of generations are set to 100 and 90 for the centrifugal pump design, 100 and 120 for the multistage pump design. Unbiased initial population is generated by randomly spreading solutions over the entire design space in consideration.

PUMP PERFORMANCE EVALUATION

Total head and required input power of pump design candidates are evaluated by using a one-dimensional meanline pump flow modeling method[14], which provides a fast capability for modeling turbopumps within rocket engines. The components of the inlet and exit fluid velocity triangles are calculated at the hub, mean and tip locations along the rotor blades. The meridional velocity of the fluid at the rotor leading edge root-mean-square diameter C_{M1} [ft/sec] is defined by equation (4).

$$C_{M1} = \frac{144m}{\rho_1 A_1} \tag{4}$$

where

m: Mass flow [lbs/sec]

ρ_1: Fluid density at leading edge [lbs/ft^3]

A_1: Flow area at leading edge [inch^2]

Flow area is calculated from the input flow path dimensions.

$$A = \lambda \left[\pi B \left(R_{hub} + R_{tip} \right) - block \right] \tag{5}$$

where

λ: Boundary layer blockage factor

B: Blade span from hub to tip [inch]

R_{hub}: Radial distance from pump centerline at hub [inch]

R_{tip}: Radial distance from pump centerline at tip [inch]

The metal blockage of the rotor *block* is calculated by eq. (6).

$$block = \frac{thk \cdot B \cdot Z}{\sin \beta} \tag{6}$$

where

thk: Normal blade thickness [inch]

Z: Blade number

β: Relative angle from tangential [degree]

The tangential component of velocity entering the rotor is calculated in terms of the swirl angle of the flow α_1 by equation (7).

$$C_{U1} = C_{M1} / \tan(\alpha_1) \tag{7}$$

The meridional and tangential components of absolute fluid velocity at the rotor trailing edge are calculated by equations (8) and (9).

$$C_{M2} = \frac{144 \, m}{\rho_2 \, A_2} \tag{8}$$

$$C_{U2} = U_2 + W_{U2} \tag{9}$$

where

ρ_2: Fluid density at trailing edge [lbs/ft^3]

A_2: Flow area at trailing edge [inch^2]

U_2: Blade tangential velocity at trailing edge [ft/sec]

W_{U2}: Tangential component of relative fluid velocity at trailing edge [ft/sec]

Flow area at trailing edge is calculated by eq. (5). The blade tangential velocity U and tangential component of the fluid relative velocity W_{U2} are given by equations (10) and (11), respectively.

$$U = \frac{2\pi \cdot R \cdot N}{720} \tag{10}$$

$$W_{U2} = C_{M2} \cdot \tan \beta_2 + U_2 (1 - \sigma) \tag{11}$$

where

R: Radial distance from pump centerline [inch]

N: Shaft rotative speed [rpm]

β_2: Relative angle from tangential at trailing edge [degree]

The slip factor σ is defined by

$$\sigma = 1 - \frac{slip}{U_2} \tag{12}$$

The slip is the difference between the theoretical and absolute fluid tangential velocities. For centrifugal impellers, Pfleiderer correlation to geometry[15] is used to calculate the slip factor σ. A default slip factor of 0.95 is used for inducers.

The head rise through the rotor is calculated iteratively from the Euler turbine equation coupled with empirical correlations for rotor efficiency

$$H_2 = \frac{\left(U_2 \cdot C_{U2} - U_1 \cdot C_{U1} \right)}{g_c} \cdot \eta_{hyd} \tag{13}$$

where

H_2: Head rise through the rotor [ft]

η_{hyd}: Rotor hydraulic efficiency

g_c: Gravitational constant, 32.174[lbm-ft/lbf-sec^2]

The rotor hydraulic efficiency is obtained from empirical correlations to rotor-specific speed[17]. The total pressure and static pressure at the rotor exit are estimated from the rotor head rise by equations (14) and (15).

$$P_{t2} = \frac{H_2 \cdot \rho_{1-2}}{144} + P_{t1} \tag{14}$$

$$P_{s2} = P_{t2} - \frac{C_2^2 \cdot \rho_2}{2 \cdot 144 \cdot g_c} \qquad (15)$$

where

P_{t1}: Total pressure at the leading edge [psia]

P_{t2}: Total pressure at the trailing edge [psia]

ρ_{1-2}: Average density of the fluid from the leading edge to the trailing edge [lbs/ft^3]

P_{s2}: Static pressure at the trailing edge [psia]

Fluid absolute velocity at trailing edge C_2 [ft/sec] is defined by

$$C_2 = \sqrt{C_{M2}^2 + C_{U2}^2} \qquad (16)$$

Total pressure at the discharge of the last stage P_{t4} [psia] is given by the following equation

$$P_{t4} = P_{t2} - \omega_{2-4} \cdot (P_{t2} - P_{s2}) \qquad (17)$$

where the design point total pressure loss coefficient of the diffusion system is assumed to be known and is input in terms of a normalized loss coefficient ω_{2-4}. The total head rise through pump is calculated by

$$H_4 = \frac{144 \cdot (P_{t4} - P_{t1})}{\rho_{1-4}} \qquad (18)$$

where

H_4: Total head rise through pump[ft]

P_{t4}: Total pressure at the pump exit [psia]

ρ_{1-4}: Average density of the fluid from the inlet to the discharge [lbs/ft^3]

The input power required to drive the rotor is calculated from the head rise through the rotor, mass flow, rotor hydraulic efficiency, mechanical efficiency, volumetric efficiency and disk pumping loss as

$$input = \left(\frac{m \cdot H_2}{\eta_{hyd} \cdot \eta_{vol}} + PL_{disk} \right) \cdot \frac{1}{\eta_{mech}} \qquad (19)$$

where

$input$: Input power [hp]

η_{mech}: Mechanical efficiency

η_{vol} : Volumetric efficiency

PL_{disk}: Disk Pumping loss [hp]

The mechanical efficiency is assumed to be 0.98 and the volumetric efficiency is based on internal leakages and is expressed as the ratio of leakage to the inlet flow. The disk pumping loss is calculated from empirical correlations to geometry, fluid density at rotor trailing edge, and the shaft rotative speed[16]. During the calculation, local static pressure at the rotor tip is compared to the local vapor pressure to check for the cavitation inception point.

To estimate off-design total head and required input power, the empirically derived variation of slip factor and rotor efficiency as a function of flow-speed ratio F is used. Correction factor is also applied to the total pressure loss coefficient of the diffusion system as a function of loading parameter L.

$$\frac{\sigma}{\sigma_{design}} = 1.534988 - 0.6681688 \cdot F + 0.077472 \cdot F^2 + 0.0571508 \cdot F^3 \qquad (20)$$

$$\frac{\eta_{hyd}}{\eta_{hyd,design}} = 0.86387 + 0.3096 \cdot F - 0.14086 \cdot F^2 - 0.029265 \cdot F^3 \qquad (21)$$

$$\frac{\omega}{\omega_{design}} = 1.8151 - 1.83527 \cdot L + 0.8798 \cdot L^2 + 0.18765 \cdot L^3 \qquad (22)$$

The loading parameter is defined in terms of the velocities at the vaneless diffuser exit and the velocity at the diffusion system throat.

$$L = \frac{C_{throat}}{\sqrt{C_{U3}^2 + C_{M3}^2}} \qquad (23)$$

where

C_{throat}: Fluid absolute velocity at the diffusion system throat [ft/sec]

C_{U3}: Tangential component of fluid absolute velocity at vaneless diffuser exit [ft/sec]

C_{M3}: Meridional component of fluid absolute velocity at vaneless diffuser exit [ft/sec]

The velocity at the diffusion system throat is defined by the equations (24) and (25).

$$C_{M3} = \frac{144m}{\rho_3 A_3} \qquad (24)$$

$$C_{U3} = (1 - \varpi_{2-3}) \cdot C_{U2} \cdot \frac{R2}{R3} \qquad (25)$$

where the pressure loss coefficient at the diffuser exit ω_{2-3} is assumed to be 0.1. Fluid velocity at the throat is given by the equation (26).

$$C_{throat} = \frac{144m}{\rho_3 A_{throat}} \qquad (26)$$

CENTRIFUGAL PUMP DESIGN

First, redesign of a single-stage centrifugal pump, M-1 oxygen scaled tester is demonstrated. Objectives of the present design problem are maximization of total head and minimization of input power at a design point. These objectives are competing and therefore the solution to this optimization problem is Pareto-optimal solutions.

The design point is shaft rotative speed of 5,416.7[rpm], total temperature of the fluid entering the pump of 545 [Rankine], total pressure of the fluid entering the pump of 50.0 [psia], and mass flow into the pump of 188.7 [lbm/sec].

Design parameters are rotor leading edge tip radius (R_{tip1}), rotor trailing edge radius (R_2), volute tongue radius (R_3), blade span at trailing edge (B_2), blade span at volute tongue (B_3), axial length of the blade at the root-mean-square diameter (S), number of blades (Z_n), blade thickness (thk), blade trailing edge angle at the hub, root-mean-square radius, and tip (β_{hub}, β_{mid}, β_{tip}) as shown in Fig. 3.

Table 1 presents present design spaces.

Total head and input power of Pareto-optimal designs, original design, and all other design candidates are illustrated in Fig. 4. Designs that have cavitation are eliminated from the figure. Present Pareto-optimal solutions successfully displays tradeoff information between maximization of the total head and minimization of the input power. Such tradeoff information is very helpful to a higher-level decision-maker in selecting a design with other considerations. Among the Pareto-optimal solutions, some designs outperform the original design in the total head while reducing the input power by 1%.

Figure 5 compares overall performance maps of the original design, the highest total head design, the lowest input power design, and a compromised design that overcomes the original design in both objectives. Moreover, the compromised design is seen to improve the exit pressure in all off-design conditions. The design parameters of these designs are shown in Table 2.

The absolute flow velocity at rotor exit hub is shown in Fig. 6. This figure indicates the optimum designs have small exit flow velocity, which contributes to minimizing the total pressure loss in the diffusion system. By minimizing the total pressure loss in the diffusion system, designs can improve their total head rise. To minimize the exit flow velocity, the optimum designs have small slip factor values, i.e., large slip than others. Actually, all three optimum designs in Table 2 have small axial length, while the high head design and the compromised design maximize R_2 to increase slip due to the inertial effect (Low input design minimize R_2 to minimize input power). The low input design and the compromised design also minimize their blade angle at hub and tip to reduce absolute fluid velocity at rotor exit (the high head design maximize blade trailing edge angles to improve its total head). However, it is known that non-uniform radial velocity around the periphery of the impeller due to large slip degrades its head rise. Therefore, this effect should be counted in the future study.

Figure 7 shows the total pressure loss coefficient of the diffusion system of the designs. Pareto-optimal solutions successfully minimize it to increase their total head rise. According to these detailed observations of the results, present MOEA obtained reasonable Pareto-optimal solutions, which ensure the feasibility of the present design optimization approach in rocket engine pump designs.

MULTISTAGE PUMP DESIGN

Next, present design optimization method is applied to the redesign of RL10A-3-3A liquid oxygen pump consisting of one inducer and a single centrifugal impeller, followed by a vaneless diffuser and conical exit volute. The objectives are maximization of total head and minimization of input power at the design point, which is shaft rotative speed of 12,900[rpm], total temperature of the fluid entering the pump of 175 [Rankine], total pressure of the fluid entering the pump of 40.0 [psia], and mass flow into the pump of 40.0 [lbm/sec]. Design parameters and the corresponding parameter ranges are shown in Fig. 8 and Table 3, respectively.

Figure 9 shows total head and input power of Pareto-optimal designs, original design, and all other design candidates that have no cavitation. Though this design optimization problem involves two stages and a large number of design parameters, the present MOEA finds reasonable Pareto-optimal solutions including some designs that improve both total head and input power by as much as 1%.

Figure 10 shows overall performance maps of the original design and optimized designs. The compromised design improves the exit pressure in all off-design conditions. The design parameters of these designs are shown in Table 4.

Figures 11 and 12 illustrate the head rise and the required input power of the first and the second stages. Because the exit of the first stage connects with the inlet of the second stage directly, the relation between the head rise and input power becomes linear. The optimum designs increase their head rise through the first stage because the slope of the curve consisting of Pareto-optimal solutions in Fig. 12 is steeper than that of the line in Fig. 11. To increase the head rise through the first stage, the highest head design and the compromised design increase R_{tip}, β_{2hub}, β_{2rms}, and β_{2tip}.

Another interesting thing is that the second stages of the Pareto-optimal designs are not optimal by themselves, especially in the high head region. This is due to the nonlinear interactions between the first and the second stages, which make a multistage pump design very difficult.

Figure 13 shows fluid velocity at rotor exit hub. The Pareto-optimal designs have a small fluid velocity at exit like the single stage pump design. However, the optimum designs that have the total head of 950-1200 inches do not

minimize their total head. This is probably due to complicated interactions between the first and second stages.

Figure 14 is the total pressure loss coefficient of the designs. This figure is also interesting because the optimal designs in low total head region minimize their total pressure loss coefficient but the optimal designs in the high total head region maximize it. More work is necessary to understand the multistage pump designs.

SUMMARY

In the present study, a design optimization method for cryogenic rocket engine turbopumps has been developed. Multiobjective Evolutionary Algorithm is used for the multiobjective optimization of pump designs. Performances of design candidates are evaluated by using the meanline pump flow modeling method, which is based on the Euler turbine equation coupled with empirical correlations for rotor efficiency.

To demonstrate the feasibility of the present approach, single stage centrifugal pump design and multistage pump design optimizations are presented. In both cases, present method obtains reasonable Pareto-optimal solutions that include designs outperforming the original design in total head as well as input power by 1%. Detailed observation of the design results also reveals some important design policies in turbopump design of cryogenic rocket engines. These results ensure the feasibility of EA-based design optimization method in this field.

REFERENCES

[1] Hicks, R. M., Murman, E. M., and Vanderplaats, G. N., "An Assessment of Airfoil Design by Numerical Optimization," NASA TM X-3092, Ames Research Center, Moffett Field, California, July 1974.

[2] Reuther, J., Cliff, S., Hicks, R., and van Dam, C. P., "Practical Design Optimization of Wing/Body Configurations Using the Euler Equations," AIAA paper 92-2633, 1992.

[3] Reuther, J., Jameson, A., Farmer, J., Martinelli, L., and Saunders, D., "Aerodynamic Shape Optimization of Complex Aircraft Configurations via an Adjoint Formulation," AIAA paper 96-0094, 1996.

[4] Vanderplaats, G. N., *Numerical Optimization Techniques for Engineering Design with applications,* McGraw-Hill, Inc., New York, 1984.

[5] Quagliarella, D., Periaux, J., Poloni, C., and Winter G. (Eds.), *Genetic Algorithms in Engineering and Computer Science,* John Wiley and Sons, Chichester, 1997.

[6] Powell, D. J., Tong, S. S. and Sholbick, M. M., "EnGENEous Domain Independent, Machine Learning for Design Optimization," Proceedings of the Third International Conference on Genetic Algorithms, Morgan Kaufmann Publishers, Inc., Sna Mateo, California, pp.151-159, 1989.

[7] Obayashi, S. and Takanashi, S., "Genetic Optimization of Target Pressure Distributions for Inverse Design Methods, " *AIAA Journal*, Vol. 34, No. 5, pp. 881-886, 1996.

[8] Oyama, A., "Multidisciplinary Optimization of Transonic Wing Design Based on Evolutionary Algorithms Coupled with CFD solver," European Congress on Computational Methods in Applied Sciences and Engineering, Barcelona, Spain, September 2000.

[9] Sasaki, D., Obayashi, S., Sawada, K. and Himeno, R., "Multiobjective Aerodynamic Optimization of Supersonic Wings Using Navier-Stokes Equations," *CD-ROM Proceedings of the ECCOMAS 2000,* 2000.

[10] Fonseca, C. M. and Fleming, P. J., "Genetic algorithms for multiobjective optimization: formulation, discussion and generalization", *Proceedings of the Fifth International Conference on Genetic Algorithms*, Morgan Kaufmann Publishers, Inc., San Mateo, California, pp. 416-423, 1993.

[11] Tsutsui, S. and Fujimoto, Y., "Forking Genetic Algorithms with blocking and shrinking modes (fGA)," *Proceedings of the Fifth International Conference on Genetic Algorithms*, Morgan Kaufmann Publishers, Inc., San Mateo, California, pp.206-213, 1993.

[12] Eshelman, L. J. and Schaffer, J. D., "Real-coded genetic algorithms and interval schemata," *Foundations of Genetic Algorithm 2*, Morgan Kaufmann Publishers, Inc., San Mateo, CA, pp.187-202, 1993.

[13] Booker, L. B., "Improving Search in Genetic Algorithms," *Genetic Algorithms and Simulated Annealing*, Morgan Kaufmann Publishers, Inc., San Mateo, CA, pp.61-73, 1987.

[14] Veres, J. P., "Centrifugal and Axial Pump Design and Off-Design Performance Prediction," NASA TM 106745, Lewis Research Center, Cleveland, Ohio, October 1994.

[15] Kovats, A., "Design and Performance of Centrifugal and Axial Flow Pumps and Compressors," Macmillan, New York, 1964.

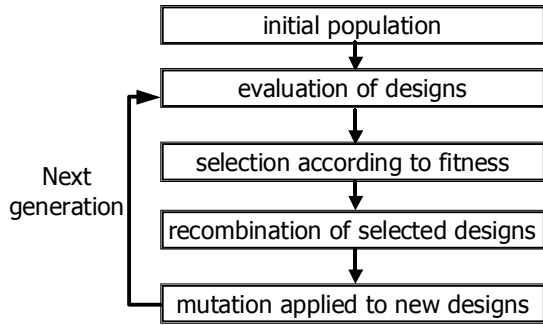[16] Stepanoff, A. J., "Centrifugal and Axial Flow Pumps: Theory, Design, and Applications," Wiley, New York, 1957.

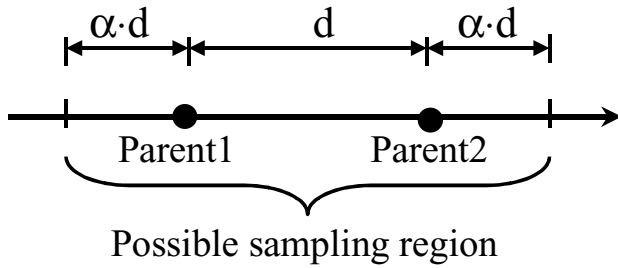**Figure 1.** Flowchart of the present evolutionary algorithm.

Figure 2. Blended crossover.

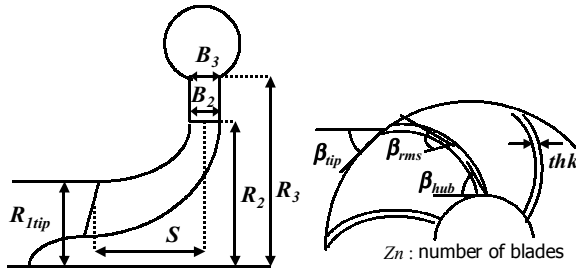**Figure 3.** Design parameters of the centrifugal pump design problem.

Table 1. Design parameter ranges of the centrifugal pump design problem.

design variables	R_{1tip} [inch]	R_2 [inch]	R_3 [inch]	B_2 [inch]	B_3 [inch]	S [inch]
Upper boundary	4.00	5.60	6.20	0.85	1.00	4.30
Lower boundary	3.40	5.00	5.60	0.70	0.85	3.70

| design variables	β_{hub} [degs.]	β_{ms} [degs.]	β_{tip} [degs.]	thk [inch]	Z_n
Upper boundary	25.0	25.0	25.0	0.03	6
Lower boundary	45.0	45.0	45.0	0.10	18
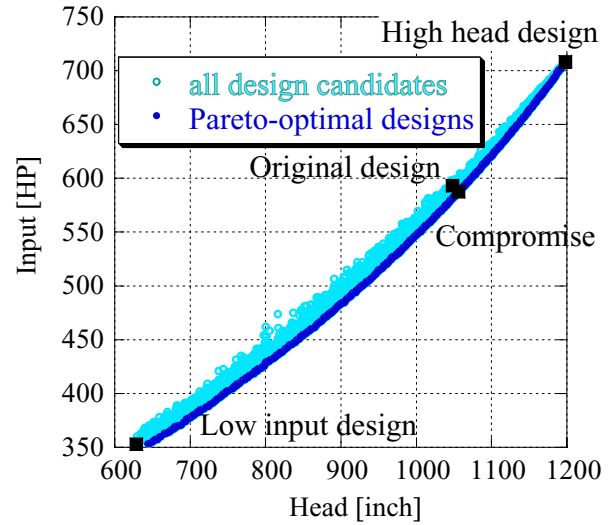
Figure 4. Objective function values of the centrifugal pump designs.
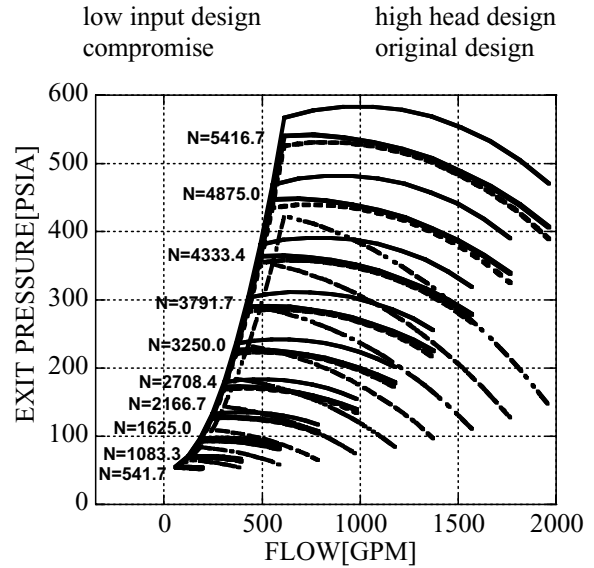
Figure 5. Pump overall performance map.

Table 2. Pareto-optimal designs of the centrifugal pump design problem.

design variables	R_{1tip} [inch]	R_2 [inch]	R_3 [inch]	B_2 [inch]	B_3 [inch]	S [inch]
High head design	3.50	5.60	6.05	0.846	0.871	3.74
Low input design	3.71	5.00	6.08	0.701	0.859	3.74
Compromised design	3.92	5.59	5.63	0.730	0.878	3.76
Original design	3.66	5.34	5.91	0.814	0.908	4.00

design variables	β_{hub} [degs.]	β_{ms} [degs.]	β_{tip} [degs.]	thk [inch]	Z_n
High head design	44.9	36.0	44.6	0.100	18
Low input design	25.3	33.2	26.1	0.065	6
Compromised design	26.7	37.2	26.4	0.042	7
Original design	35.0	35.0	35.0	0.050	12
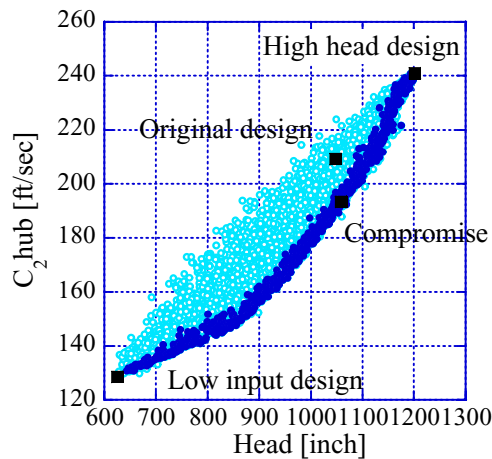
Figure 6. Flow velocity at second stage exit hub.
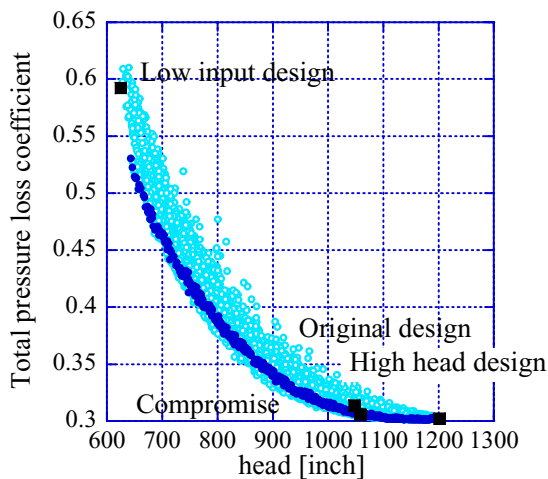
Figure 7. Total pressure loss coefficient of the centrifugal pump designs.
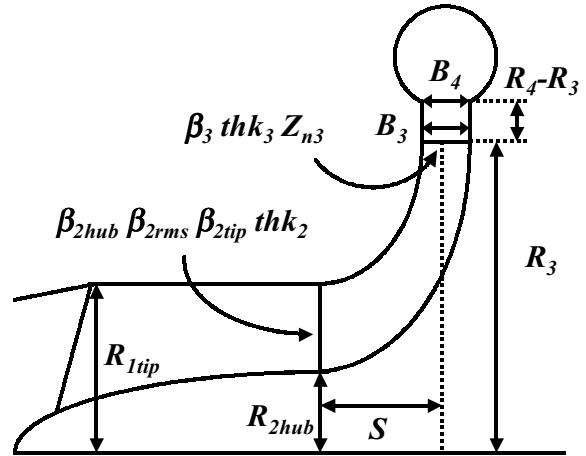
Figure 8. Design parameters of the multistage pump design problem.

Table 3. Design parameter ranges of the multistage pump design problem.

<1st stage>

design variables	R_{tip} [inch]	R_{2hub} [inch]	β_{2hub} [degs.]	β_{2ms} [degs.]	β_{2tip} [degs.]	thk_2 [inch]
Upper boundary	1.18	0.53	50.0	40.0	35.0	0.08
Lower boundary	1.08	0.43	35.0	25.0	20.0	0.03

<2nd stage>

design variables	R_2 [inch]	(R_4-R_3) [inch]	B_2 [inch]	B_3 [inch]	thk_3 [inch]	S [inch]	Z_{n3}	β_3 [degs.]
Upper boundary	2.20	0.15	0.35	0.50	0.08	1.00	16	90.0
Lower boundary	2.00	0.05	0.15	0.30	0.03	0.80	8	60.0
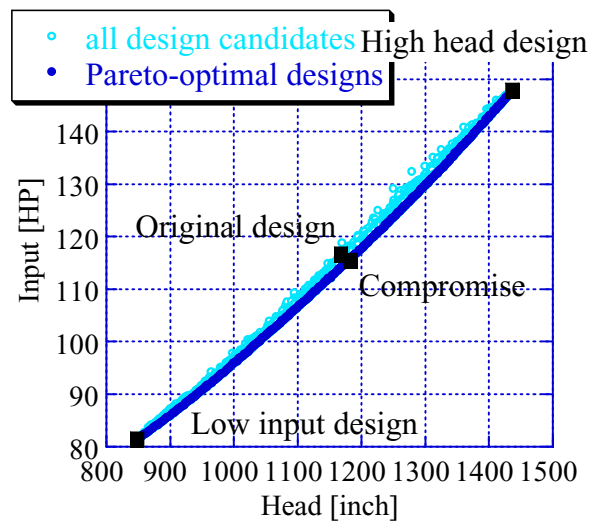
Figure 9. Objective function values of the multistage pump designs.
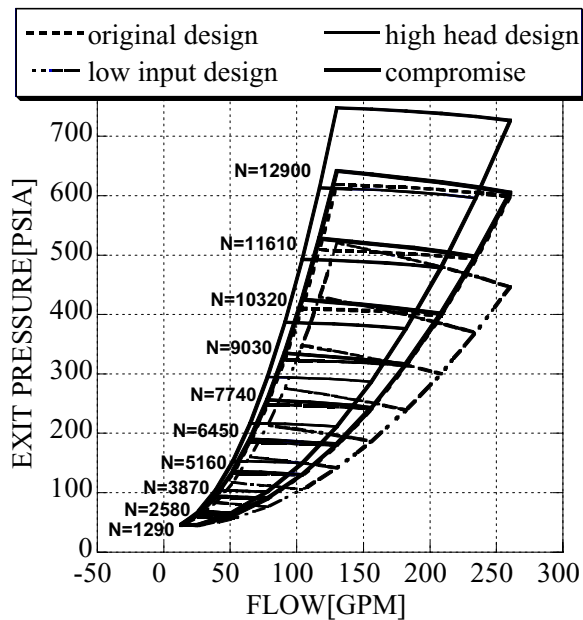
Figure 10. Pump overall performance map.

Figure 11. First stage performances of the multistage pump designs.

Table 4. Pareto-optimal designs of the multistage pump design problem.

<1st stage>

design variables	R_{tip} [inch]	R_{2hub} [inch]	β_{2hub} [degs.]	β_{2ms} [degs.]	β_{2ip} [degs.]	thk_2 [inch]
High head design	1.17	0.517	49.9	38.5	34.9	0.0788
Low input design	1.17	0.525	42.9	37.3	28.0	0.0378
Compromised design	1.17	0.514	48.3	40.0	33.4	0.0520
Original design	1.13	0.480	43.0	27.3	21.6	0.0400

<2nd stage>

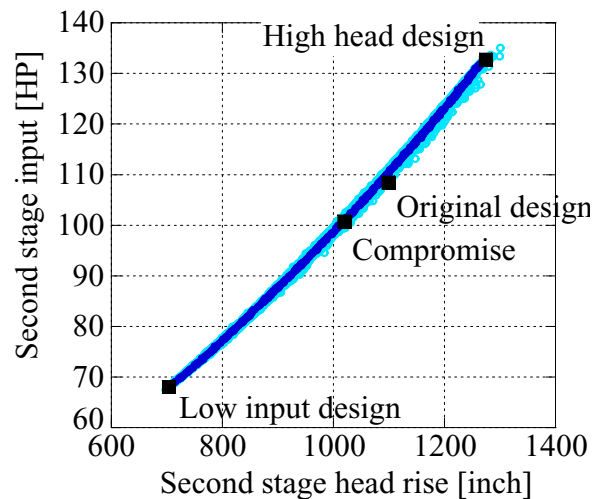| design variables	R_3 [inch]	(R_4-R_3) [inch]	B_3 [inch]	B_4 [inch]	thk_3 [inch]	S [inch]	Z_{n3}	β_3 [degs.]
High head design	2.20	0.1350	0.340	0.301	0.0311	0.855	16	87.4
Low input design	2.00	0.0548	0.152	0.393	0.0798	0.804	8	64.4
Compromised design	2.16	0.0608	0.333	0.370	0.0439	0.812	9	77.8
Original design	2.10	0.0950	0.251	0.400	0.0300	0.878	12	90.0

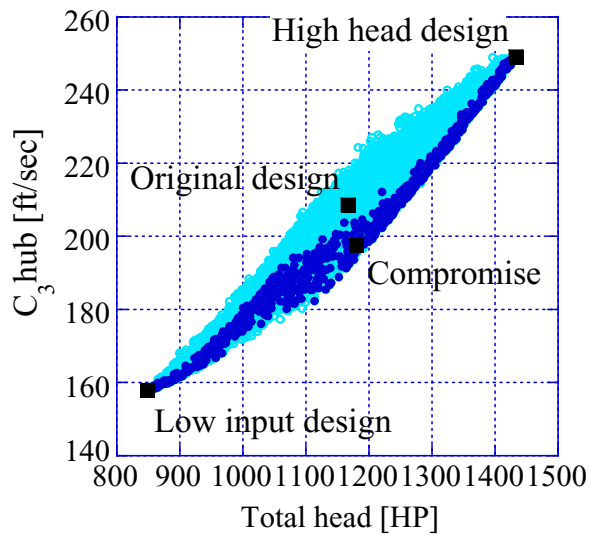**Figure 12.** Second stage performances of the multistage pump designs.

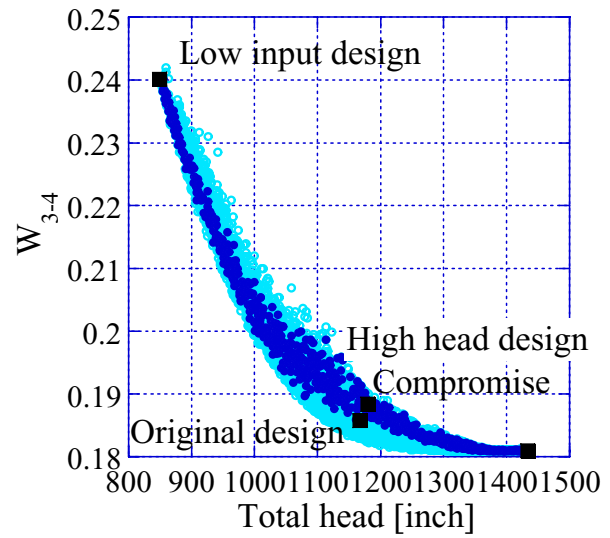**Figure 13.** Flow velocity at second stage exit hub.

Figure 14. Total pressure loss coefficient of the multistage pump designs.

REPORT DOCUMENTATION PAGE			Form Approved OMB No. 0704-0188

1. AGENCY USE ONLY (*Leave blank*)	2. REPORT DATE August 2001	3. REPORT TYPE AND DATES COVERED Technical Memorandum	

4. TITLE AND SUBTITLE

Multiobjective Optimization of Rocket Engine
Pumps Using Evolutionary Algorithm

5. FUNDING NUMBERS

WU–708–87–13–00

6. AUTHOR(S)

Akira Oyama and Meng-Sing Liou

7. PERFORMING ORGANIZATION NAME(S) AND ADDRESS(ES)

National Aeronautics and Space Administration
John H. Glenn Research Center at Lewis Field
Cleveland, Ohio 44135–3191

8. PERFORMING ORGANIZATION REPORT NUMBER

E–12923

9. SPONSORING/MONITORING AGENCY NAME(S) AND ADDRESS(ES)

National Aeronautics and Space Administration
Washington, DC 20546–0001

10. SPONSORING/MONITORING AGENCY REPORT NUMBER

NASA TM—2001-211082
AIAA–2001–2581

11. SUPPLEMENTARY NOTES

12a. DISTRIBUTION/AVAILABILITY STATEMENT

Unclassified - Unlimited
Subject Categories: 05 and 07   Distribution: Nonstandard

Available electronically at http://gltrs.grc.nasa.gov/GLTRS

This publication is available from the NASA Center for AeroSpace Information, 301–621–0390.

12b. DISTRIBUTION CODE

13. ABSTRACT *(Maximum 200 words)*

A design optimization method for turbopumps of cryogenic rocket engines has been developed. Multiobjective Evolutionary Algorithm (MOEA) is used for multiobjective pump design optimizations. Performances of design candidates are evaluated by using the meanline pump flow modeling method based on the Euler turbine equation coupled with empirical correlations for rotor efficiency. To demonstrate the feasibility of the present approach, a single stage centrifugal pump design and multistage pump design optimizations are presented. In both cases, the present method obtains very reasonable Pareto-optimal solutions that include some designs outperforming the original design in total head while reducing input power by 1 percent. Detailed observation of the design results also reveals some important design criteria for turbopumps in cryogenic rocket engines. These results demonstrate the feasibility of the EA-based design optimization method in this field.

14. SUBJECT TERMS

Multiobjective optimization; Evolutionary algorithm; Pumps

15. NUMBER OF PAGES
16

16. PRICE CODE

17. SECURITY CLASSIFICATION OF REPORT Unclassified	18. SECURITY CLASSIFICATION OF THIS PAGE Unclassified	19. SECURITY CLASSIFICATION OF ABSTRACT Unclassified	20. LIMITATION OF ABSTRACT